

Dissecting the Wjj Anomaly: Diagnostic Tests of a Leptophobic Z' *

J.L. Hewett and T.G. Rizzo[†]

SLAC National Accelerator Laboratory,
2575 Sand Hill Rd, Menlo Park, CA 94025, USA

Abstract

We examine the scenario where a leptophobic Z' boson accounts for the excess of events in the Wjj channel as observed by CDF. We assume generation independent couplings for the Z' and obtain allowed regions for the four hadronic couplings using the cross section range quoted by CDF as well as constraints from dijet production at UA2. These coupling regions translate into well-determined rates for the associated production of $Z/\gamma + Z'$ at the Tevatron and LHC, as well as $W + Z'$ at the LHC, that are directly correlated with the Wjj rate observed at the Tevatron. The Wjj rate at the LHC is large and this channel should be observed soon once the SM backgrounds are under control. The rates for $Z/\gamma + Z'$ associated production are smaller, and these processes should not yet have been observed at the Tevatron given the expected SM backgrounds. In addition, we also show that valuable coupling information is obtainable from the distributions of other kinematic variables, *e.g.*, $M_{WZ'}$, p_T^W , and $\cos\theta_W^*$. Once detected, these associated production processes and the corresponding kinematic distributions examined here will provide further valuable information on the Z' boson couplings.

*Work supported by the Department of Energy, Contract DE-AC02-76SF00515

[†]e-mail: hewett, rizzo@slac.stanford.edu

1 Introduction and Background

The CDF Collaboration has reported the observation of an excess of events [1] in the $\ell\nu jj$ channel with a statistical significance of 3.2σ corresponding to 4.3 fb^{-1} of integrated luminosity. Recently, CDF has included an additional 3 fb^{-1} to their data sample [2], for a total of 7.3 fb^{-1} , and the significance of this anomaly has grown to $\sim 4.8\sigma$ ($\sim 4.1\sigma$ including systematics). This is now a serious situation. An examination of the m_{jj} distribution for these events reveals a peak that is compatible with Standard Model (SM) $WW + WZ$ production, as well as a second peak that is compatible with a new resonance at $m_{jj} \sim 150 \text{ GeV}$.

This state of affairs has gathered much attention, even before the inclusion of the additional data sample. Skeptics have been concerned about the detailed shape of the Monte Carlo simulation modeling of the SM background, the jet-energy scale, as well as possible contamination from top-quark production [3][4]. However, the CDF Collaboration has shown [2] that neither the top background nor changes to the jet-energy scale is likely to account for this excess. Optimists have offered several new physics explanations, including a new Z' boson [5] [6], technicolor [7], Supersymmetry with and without R-parity conservation [8], color octet production [9], and more [10]. More recently, the D0 Collaboration has weighed in on this anomaly [11] and does not observe a signal at the same level as claimed by CDF in a luminosity sample of 4.3 fb^{-1} . An understanding of this discrepancy between CDF and D0 has not yet been reached, and the situation most likely will only be clarified with results from the LHC. Certainly, if new physics is really present, it's cross section is most likely to be at the low end of the range discussed by CDF.

Here, we will assume the excess observed by CDF is due to new physics, and we will further examine the possibility of Z' production, $p\bar{p} \rightarrow W + Z' \rightarrow \ell\nu + jj$, as the potential source. Interestingly, we note that the CDF data shows a sharp dip, or valley, in the m_{jj} spectrum between the first peak (*i.e.*, SM $WW + WZ$ production) and the second peak (the hypothetical Z' boson); this is the behavior that one might expect due to the destructive interference between the SM W and Z and a new gauge boson [12]. Clearly, this new Z' boson must have very leptophobic couplings in order to evade direct production at LEP II as well as the Tevatron and LHC Z' Drell-Yan dilepton searches. In addition, there must be some mechanism which prohibits any significant $Z - Z'$ mixing ($\lesssim 10^{-3}$) in order to be consistent with precision electroweak data and to avoid any 'leakage' of the SM Z leptonic couplings to the Z' . CDF reports [1] that there is no particular excess of b-quarks in the events near $m_{jj} \sim 150 \text{ GeV}$, and thus we will assume that the Z' decays democratically to all kinematically accessible hadronic states, *i.e.*, the Z' has generation-independent couplings[‡].

It has been known since long ago (in preparation for the SSC) [14], that the associated production $W/Z/\gamma + Z'$ provides an excellent opportunity to perform diagnostic tests on the coupling structure of a new gauge boson. In particular, if the Z' explanation for the CDF

[‡]Note, however, that a significant b-quark content for these jets, $\lesssim 20 - 30\%$, is consistent with the existing CDF data [13, 2].

excess is correct, then one should at some point also observe $Z + Z'$ and $\gamma + Z'$ associated production. As we will show below, given the CDF result, one can make relatively definitive predictions for the rates of these processes at both the Tevatron and the LHC.

In what follows, we will perform an analysis of the possible coupling structure and strength for the Z' that is consistent with the data and will determine the allowed regions for the left- and right-handed Z' couplings. We will then be armed to compute the predictions for $W/Z/\gamma + jj$ production. We find that the rates for $Z/\gamma + jj$ are likely too small to be observed at the Tevatron with current data samples, and that a Z' in $W/Z/\gamma + jj$ could be detected at the LHC with integrated luminosities of order a few fb^{-1} once SM backgrounds are under control. We provide the most general expressions for these cross sections. We also examine the $M_{WZ'}$, as well as other, kinematic distributions and show that they can yield additional valuable coupling information, particularly for the left-handed quarks. Our main conclusion is that the allowed regions of the Z' couplings are relatively restricted, allowing for reasonably firm predictions for the associated production rates and the rates for other kinematic distributions. If the CDF anomaly is due to a new ~ 150 GeV leptophobic Z' boson, the LHC should confirm this signal relatively soon.

2 Analysis

We define the couplings of the Z' to the SM quarks in a manner similar to that for the conventional SM Z boson,

$$\mathcal{L} = \frac{g}{2c_W} \bar{q} \gamma^\mu (v'_q - a'_q \gamma_5) q Z'_\mu \quad (q = u, d), \quad (1)$$

in order to make contact with our earlier analyses [12, 14]. It will also be convenient to define the chiral coupling combinations $u_{L,R} = v'_u \pm a'_u$ (and similarly for $u \rightarrow d$) for the analysis below. For simplicity, and to avoid possible issues with Flavor Changing Neutral Currents (FCNC), we will assume that these couplings are generation-independent; this assumption has very little (if any) direct impact in what follows as it is essentially only the Z' couplings to the first generation quarks that determine its production cross sections at the Tevatron and LHC. We will, however, return to this point later below when discussing the Z' total decay width.

Since the observed excess is in the proposed $W^\pm + Z'$ channel, let us first examine the differential cross section for this process; it is easily obtained from the expressions in the original Refs. [15],[16] which describe the corresponding SM process with suitable simple modifications:

$$\frac{d\sigma}{dz} = K_W \frac{G_F^2 M_Z^4}{48\pi \hat{s}} (2c_W^2) \beta_W \left[(u_L - d_L)^2 X + \left[u_L^2 \frac{\hat{s}^2}{\hat{u}^2} + d_L^2 \frac{\hat{s}^2}{\hat{t}^2} \right] Y + 2u_L d_L (M_W^2 + M_{Z'}^2) \frac{\hat{s}}{\hat{u}\hat{t}} \right], \quad (2)$$

where K_W (taken to be 1.3 in our numerical analysis) is a NLO K-factor, $c_W = \cos \theta_W$, $\beta_W(z)$ is the speed of the W boson in the center of mass (CM) frame, z is the CM scattering angle $\cos \theta^*$, $Y = (\hat{u}\hat{t} - M_W^2 M_{Z'}^2)/\hat{s}^2$ and the quantity X is given by the expression

$$X = \frac{1}{M_W^2 M_{Z'}^2} \left[\frac{1}{4}(\hat{u}\hat{t} - M_W^2 M_{Z'}^2) + \frac{1}{2}(M_W^2 + M_{Z'}^2)\hat{s} \right]. \quad (3)$$

Since the SM W is purely left-handed, the right-handed couplings of the Z' to the SM quarks are projected out in this amplitude so that only the left-handed couplings of both u and d appear in this expression for the cross section. It is important to note that for large values of \hat{s} , X behaves as $\sim \hat{s}^2/M_W^2 M_{Z'}^2 \gg 1$ and can provide a very significant cross section enhancement when $u_L \neq d_L$ as was noted numerically by some previous authors [5],[6],[14]. In contrast, the other terms in the cross section are of order unity (or parametrically smaller) in the same limit. As we will see below, the presence of this term will allow for a large $W + Z'$ production rate, without necessarily enhancing the corresponding $Z/\gamma + Z'$ cross sections. However, we note that the possibility of $u_L \neq d_L$ implies that the group generator, Q' , to which the Z' couples does not commute with the usual $SU(2)_L$ isospin generators, *i.e.*, $[Q', T_i] \neq 0$. This can have a number of implications elsewhere [17].

Requiring that the Z' decays only to two jets, integration of the above expression over $z = \cos \theta^*$ and the relevant parton densities leads to the numerical value for the (pre-cut) $W + Z'$ cross sections at the Tevatron and LHC for arbitrary couplings given by

$$\begin{aligned} \sigma_{W \pm Z'} &\simeq 4.945 (u_L - d_L)^2 + 0.719 (u_L^2 + d_L^2) + 5.083 u_L d_L \quad (\text{TeVatron}), \\ \sigma_{W \pm Z'} &\simeq 28.61 (u_L - d_L)^2 + 4.029 (u_L^2 + d_L^2) + 21.65 u_L d_L \quad (\text{LHC}). \end{aligned} \quad (4)$$

These results explicitly show the enhancement arising in the case of $u_L \neq d_L$. In performing these numerical calculations, and the ones found below, we make use of the CTEQ6.6M parton density functions [18]. Since the apparent excess in the Tevatron $W + Z'$ cross section is observed [1], prior to acceptance and analysis cuts, to be in the range of $\sim 1 - 4$ pb, this results in an ellipse of potentially allowed values in the $u_L - d_L$ plane[§]. This is displayed in the top panel of Fig. 1, assuming $M_{Z'} = 150$ GeV; in this figure we show the allowed ellipses for $W + Z'$ cross section values ranging from 1.5-4.0 pb. Of course, given the results from D0, the lower end of this range will be likely to be of interest to us in what follows.

Of course, a leptophobic Z' boson will also be produced directly and contribute to dijet production and may be observed as a resonance in the dijet invariant mass spectrum. Due to kinematics, the data from $Spp\bar{S}$ has the best signal to background ratio for searches in the dijet channel in this low mass region. UA2 [19] performed such a search in the dijet channel and constrained the cross section to be less than roughly $\simeq 150$ pb for a ~ 150 GeV resonance. This places an additional constraint on the Z' couplings that needs to be satisfied. Employing the narrow width approximation (which we will justify below), the dijet

[§]The exact result is somewhat sensitive to acceptance corrections.

rate induced by a Z' at UA2 (recall the CM energy for the $Spp\bar{S}$ was 630 GeV) resulting from the process $q\bar{q} \rightarrow Z' \rightarrow jj$ can be written numerically as

$$\sigma_{UA2} \simeq \frac{1}{2} [773 (u_L^2 + u_R^2) + 138 (d_L^2 + d_R^2)] \text{ (pb)}, \quad (5)$$

making use of the same procedure and assumptions as above. Given this result and the UA2 bound on the cross section, the *largest* corresponding constraint ellipse that can be drawn in the $u_L - d_L$ plane denoting the UA2 allowed region is obviously obtained when the Z' has only left-handed quark couplings, *i.e.*, $u_R = d_R = 0$. This bound is shown as the red ellipse in the top panel of Fig. 1. Clearly, if non-zero values of u_R or d_R are also present, then this constraint ellipse will only *contract*. Here we note that the UA2-allowed coupling ellipse intersects the corresponding ones obtained by evaluating the $W^\pm Z'$ cross section at the Tevatron at different values of the Z' couplings depending upon the assumed value of $\sigma_{W^\pm Z'}$. Note that the simultaneous consistency of the CDF result with the UA2 dijet data forbids very large u_L couplings of either sign and allows for the possibility of $u_L \neq d_L$. The segments of these ellipses that are simultaneously allowed by both cross section constraints are highlighted in the lower panel of Fig. 1 and are color coded for comparisons with results to be shown in later figures.

For the case $u_R = d_R = 0$, the upper panel in Fig. 2 shows the predicted UA2 dijet cross section along the allowed coupling line segments of Fig. 1. The curves in this figure correspond to the upper set of arcs in Fig. 1; a corresponding set of curves can also be obtained representing the bottom arcs and is obtained by flipping the values $u_L \rightarrow -u_L$ in Fig. 2. In all cases we see that the values along the parabolic shaped curves can lead to a dijet cross section that is significantly far from the quoted upper bound. However, this still implies that the possible values of u_R, d_R must be restricted or the UA2 dijet bound would be exceeded. Of course, for any arbitrary point along these parabolas one can perform a scan of the $u_R - d_R$ plane to obtain the corresponding region which is allowed by UA2; the weakest bounds on the right-handed couplings are clearly obtained when the predicted dijet cross section is minimized. These constraints on the maximal values of the right-handed couplings are shown in the $u_R - d_R$ plane in the lower panel of Fig. 2 for various values of the Tevatron $W + Z'$ cross section. Note that while the largest $u_R - d_R$ allowed region is obtained at the minimum of the parabolas in the top panel, the region will shrink substantially at points where the dijet cross section arising from the left-handed couplings alone almost saturates the UA2 bound.

Now that we have obtained constraints on the left- and right-handed Z' couplings, let us turn to the other relevant processes for associated production, namely $Z + Z'$ and $\gamma + Z'$. In analogy with our $W^\pm + Z'$ result above, the $q\bar{q} \rightarrow Z + Z'$ differential cross section can be obtained by a suitable modification of the corresponding result in the SM given by [15] [16]

$$\frac{d\sigma}{dz} = K_Z \frac{G_F^2 M_Z^4}{48\pi \hat{s}} \beta_Z \left[(v_q + a_q)^2 q_L^2 + (v_q - a_q)^2 q_R^2 \right] P, \quad (6)$$

where $(v, a)_q$ are the couplings of the quarks to the SM Z boson, K_Z, β_Z are the K-factor

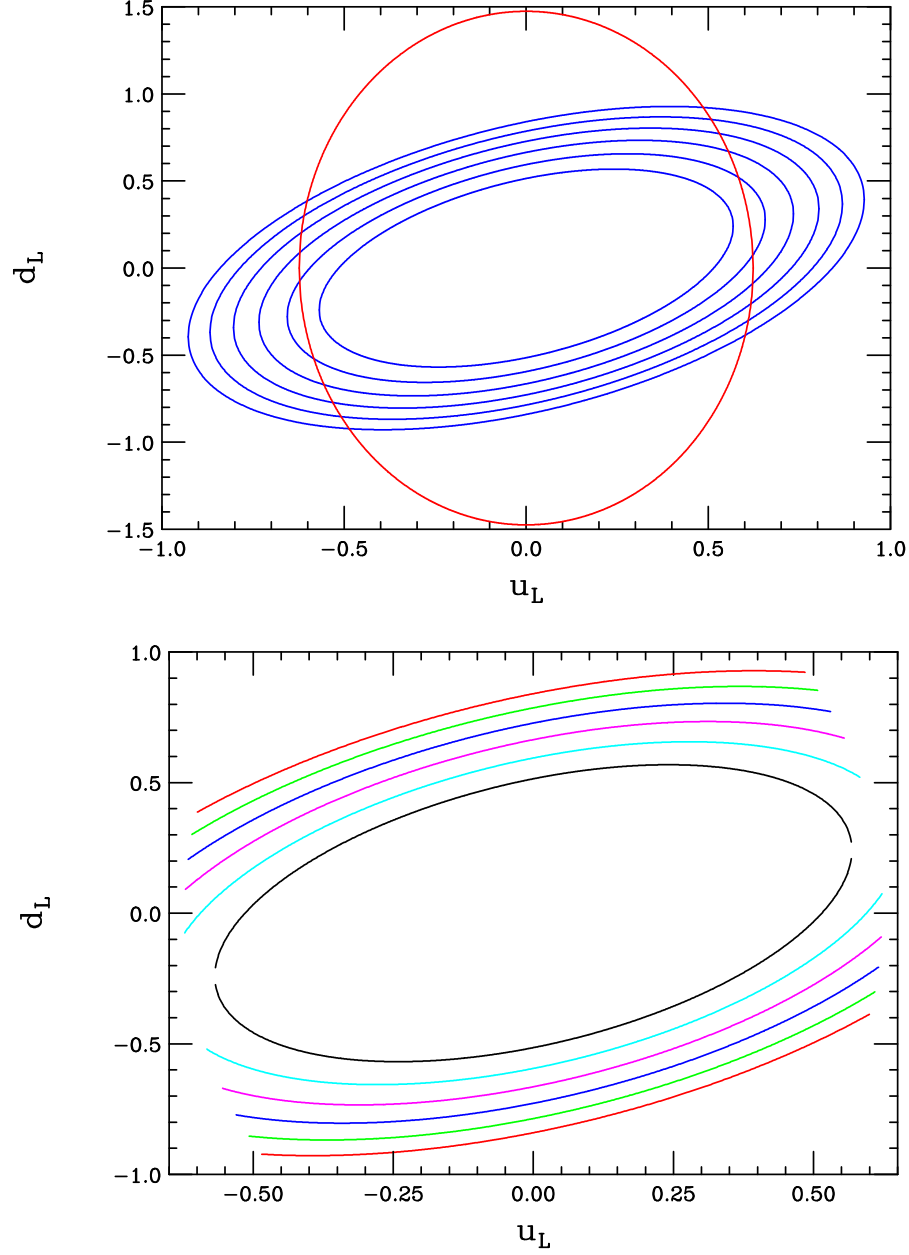


Figure 1: Top: The blue ellipses show the values of the u_L, d_L couplings leading to the Tevatron $W^\pm Z'$ cross section of (from inside out) 1.5-4.0 pb in steps of 0.5 pb. The red ellipse shows the *maximum* size of the UA2 allowed region in the $u_L - d_L$ plane. Bottom: The color-coded arcs shown here are the line segments where the Tevatron (blue) ellipses intersect and are contained within the UA2 (red) ellipse in the top panel.

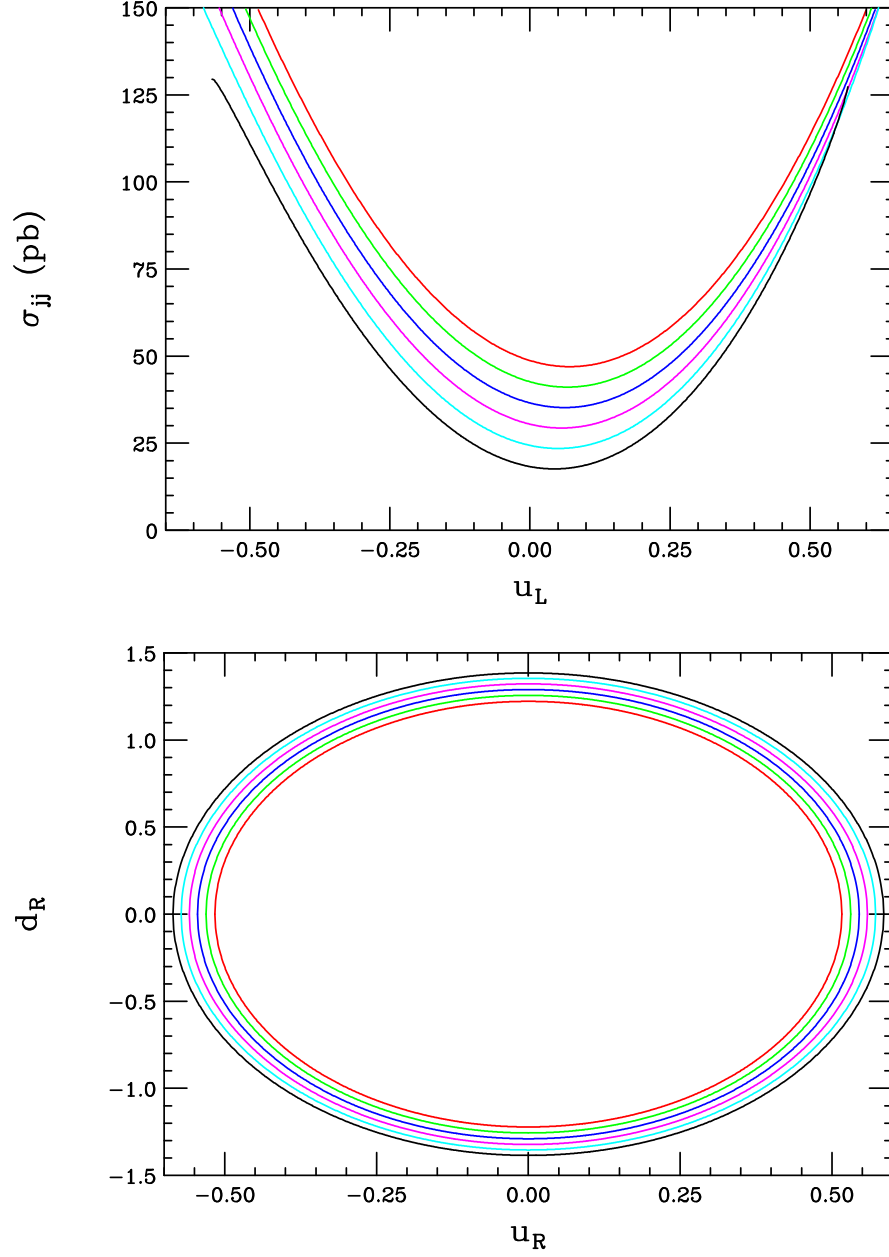


Figure 2: Top: Predicted values of the UA2 dijet cross section along the color-coded arcs for u_L, d_L as shown in the previous Figure. Note that an additional set of solutions are present when $u_L \rightarrow -u_L$ as discussed in the text. Bottom: Maximum allowed values of $u_R - d_R$ at the minima of the parabolas in the top panel. From inside out these correspond to Tevatron $W + Z'$ cross sections of 1.5, 2., 2.5, 3, 3.5 and 4 pb, respectively.

(=1.3 here) for this process and speed of the SM Z in the CM frame, and P represents the same kinematics as in the $W^\pm + Z'$ case above in the limit of equal couplings and with the replacement $M_W \rightarrow M_Z$, *i.e.*,

$$P = \left(\hat{u}\hat{t} - M_Z^2 M_{Z'}^2 \right) \left(\frac{1}{\hat{u}^2} + \frac{1}{\hat{t}^2} \right) + 2 \frac{\hat{s}(M_Z^2 + M_{Z'}^2)}{\hat{u}\hat{t}}. \quad (7)$$

Since the SM Z couplings are known, and folding in the SM Z decay to lepton pairs (with $B = 0.03366$ for e or μ and then summing over both) this expression can be numerically evaluated for arbitrary Z' couplings after integration over z and the relevant parton densities at either the Tevatron or the LHC. Writing

$$\sigma_{ZZ'} \simeq \frac{1}{4} \left[\alpha_Z u_L^2 + \beta_Z u_R^2 + \gamma_Z d_L^2 + \delta_Z d_R^2 \right], \quad (8)$$

we obtain, in units of fb and before any cuts, $\alpha_Z = 381.5(1109)$, $\beta_Z = 221(76.1)$, $\gamma_Z = 1323(166.4)$ and $\delta_Z = 44.1(5.54)$ for the case of the Tevatron(LHC). It is important to note that the SM Z leptonic branching fractions have been included here to ease comparison with experiment.

Analogously, we can obtain the corresponding numerical result for the case of the $\gamma + Z'$ final state; the analytic expression for the differential cross section can be obtained from that for $Z + Z'$ production by taking $M_Z \rightarrow 0$ in P and by a setting $v_Q \sim Q_q$ with $a_q = 0$. In this case we impose the experimental cuts $|\eta_\gamma| < 1.1(2.5)$ and $p_T^\gamma > 25(50)$ GeV at the Tevatron(LHC) and obtain numerically after integration

$$\sigma_{\gamma Z'} \simeq \frac{1}{2} \left[f_u^\gamma (u_L^2 + u_R^2) + f_d^\gamma (d_L^2 + d_R^2) \right], \quad (9)$$

where $f_u^\gamma = 767(533)$ fb and $f_d^\gamma = 72.7(114)$ fb at the Tevatron(LHC).

We are now ready to calculate the expected values of $\sigma_{ZZ',\gamma Z'}$ at both colliders. In evaluating the Z' couplings, we proceed as follows: we select a point on one of the line segments in the bottom panel of Fig. 1 which tells us the specific values of u_L, d_L . We then locate that point on the upper panel in Fig. 2 and scan over the possible values in the $u_R - d_R$ plane which are consistent with the UA2 upper bound on the dijet cross section for those u_L, d_L couplings and obtain the maximum and minimum values for both $\sigma_{ZZ',\gamma Z'}$ at the Tevatron and the LHC. The minimum values in all cases correspond, of course, to the situation when $u_R = d_R = 0$ as contributions arising from non-zero values of these couplings always add constructively. The results of this analysis for the Tevatron and LHC are shown in Fig. 3 and Fig. 4, respectively, employing the same color coding as before. We see that these cross sections are much smaller than that for $W^\pm + Z'$ at the Tevatron (as well as for the LHC) and are possibly too small to be observed at the Tevatron with present integrated luminosities given SM backgrounds. These cross sections are, of course, much larger at the LHC and should be observable with roughly 1 fb^{-1} of integrated luminosity once SM backgrounds are sufficiently understood. The predicted results for $\sigma_{W^\pm Z'}$ at the

LHC, which are independent of the possible values of u_R, d_R as was the case for the Tevatron, can be found in Fig. 5. Note that the branching fraction for the leptonic decays of the SM W are included in these results. We see that the cross section is quite large and should be detectable soon.

We learn a number of things from examining these Figures: (i) The predicted values for $\sigma_{\gamma Z', ZZ'}$ at the Tevatron (and the LHC) are always substantially lower than the corresponding ones for $\sigma_{W^\pm Z'}$. These processes should *not yet* have been observed at the Tevatron but will eventually provide a test of the Z' hypothesis once enough data accumulates at the LHC. ¶ (ii) The predicted values of $\sigma_{\gamma Z', ZZ'}$ are relatively constrained and are determined by the CDF $W + Z'$ cross section itself, as well as by the UA2 dijet constraints, except for possible NLO contributions. (iii) The $\gamma Z', ZZ'$ cross sections at the LHC and the ZZ' cross section at the Tevatron are found to be relatively insensitive to the specific values of u_R, d_R due to the rather strong constraints arising from the UA2 data. (iv) The $\gamma Z'$ process at the Tevatron could potentially be used to obtain further constraints on the values of u_R, d_R given sufficient integrated luminosity. (v) The $W^\pm Z'$ cross section at the LHC is large and is well-predicted apart from possible NLO contributions. Lastly, (vi) we see that the *ratio* of the $W^+ Z'$ and $W^- Z'$ cross sections at the LHC also has a weak coupling dependence which may also be useful as an additional handle on the left-handed quark couplings of the Z' . Thus we see that even with four free coupling parameters, the Z' explanation of the Wjj excess seen by CDF leads to a very predictive scenario that can be further tested quite soon at both the Tevatron and the LHC.

To be consistent, we need to demonstrate that our use of the narrow width approximation is valid in the Z' scenario. Essentially, it suffices to show that the Z' total width, Γ , assuming decays to only SM particles, is always substantially smaller than the CDF dijet mass resolution, $\simeq 14.3$ GeV [1], for $M_{Z'} \sim 150$ GeV. Clearly, this condition will be most difficult to satisfy when the Z' couples in a generation-independent manner to all 3 generations (as we have assumed here) instead of, *e.g.*, only to the first generation which can then lead to significant flavor physics issues. Using the Z' coupling parameter scans above, we can calculate the allowed regions for the predicted value of Γ ; the results are shown in Fig. 6, using the same color coding as before. Here we see that in the generation-independent coupling scenario, Γ always remains in the range $0.5 - 5.6$ GeV, *i.e.*, a set of values significantly below the CDF dijet mass resolution. Thus the Z' will always appear to be quite narrow and, in particular, with $\Gamma/M_{Z'} \lesssim 3.3\%$, validates our use of the narrow width approximation above. It is also of some interest to notice that the corresponding branching fractions for the decay $Z' \rightarrow b\bar{b}$, under the assumption of 3-generation coupling universality, are always found to lie in the approximate range $\sim 0 - 0.33$, which is consistent with the Wjj data from CDF [2, 13]. The coupling dependence of this branching fraction can be seen in detail in the lower panel of Fig. 6. If lower values for this branching fraction are favored this would be an indication for couplings with $|u_L| > |d_L|$.

¶In fact, their observation at the Tevatron at relatively low luminosity would likely have ruled out the Z' hypothesis.

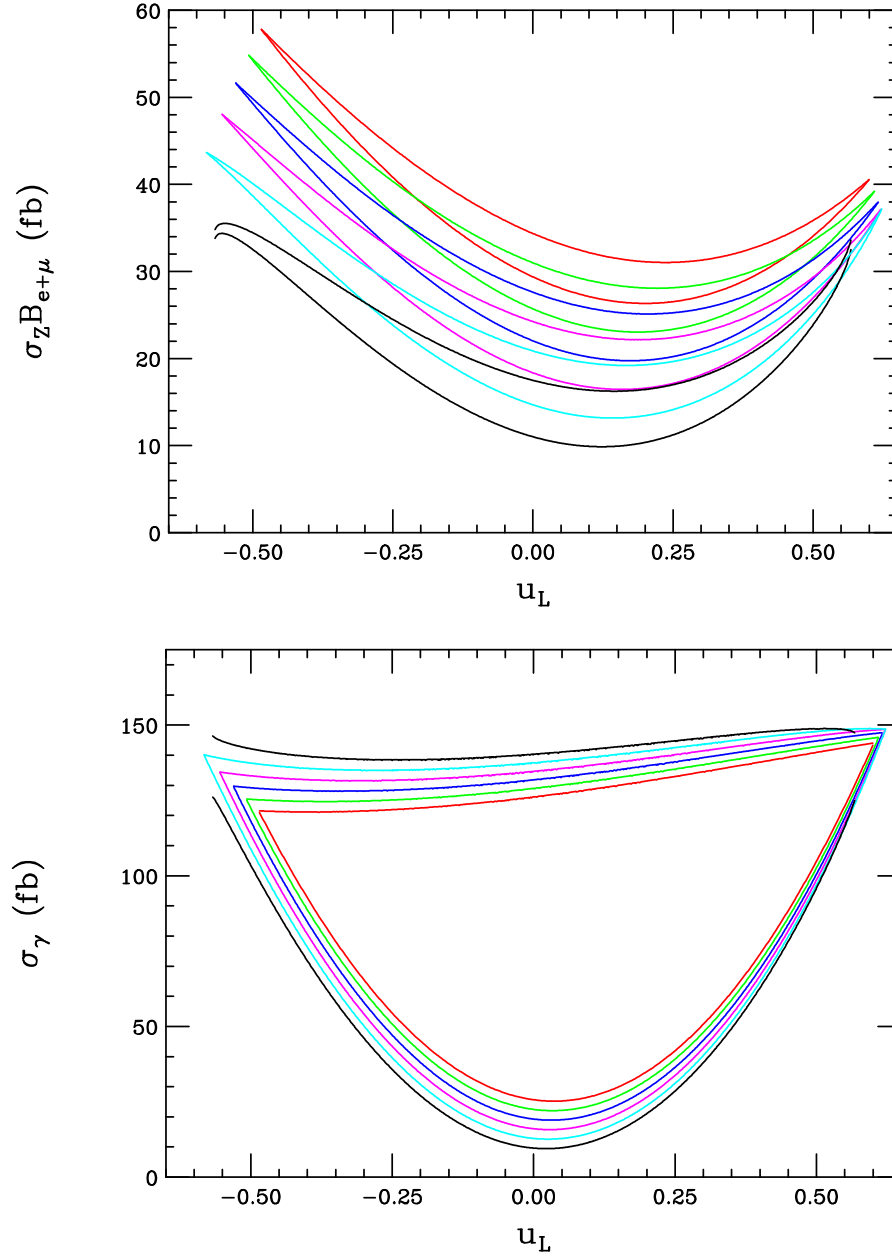


Figure 3: Predicted allowed values of the cross sections $\sigma_{ZZ',\gamma Z'}$ at the Tevatron for the parameter space regions associated with the color-coded arcs shown in the previous Figures corresponding to WZ' cross section of 1.5 – 4.0 pb at the Tevatron. The allowed region lies within the areas outlined in a specific color. For the ZZ' final state the branching fractions for leptonic decay of the Z are included. Note that an additional region exists with $u_L \rightarrow -u_L$ as discussed above.

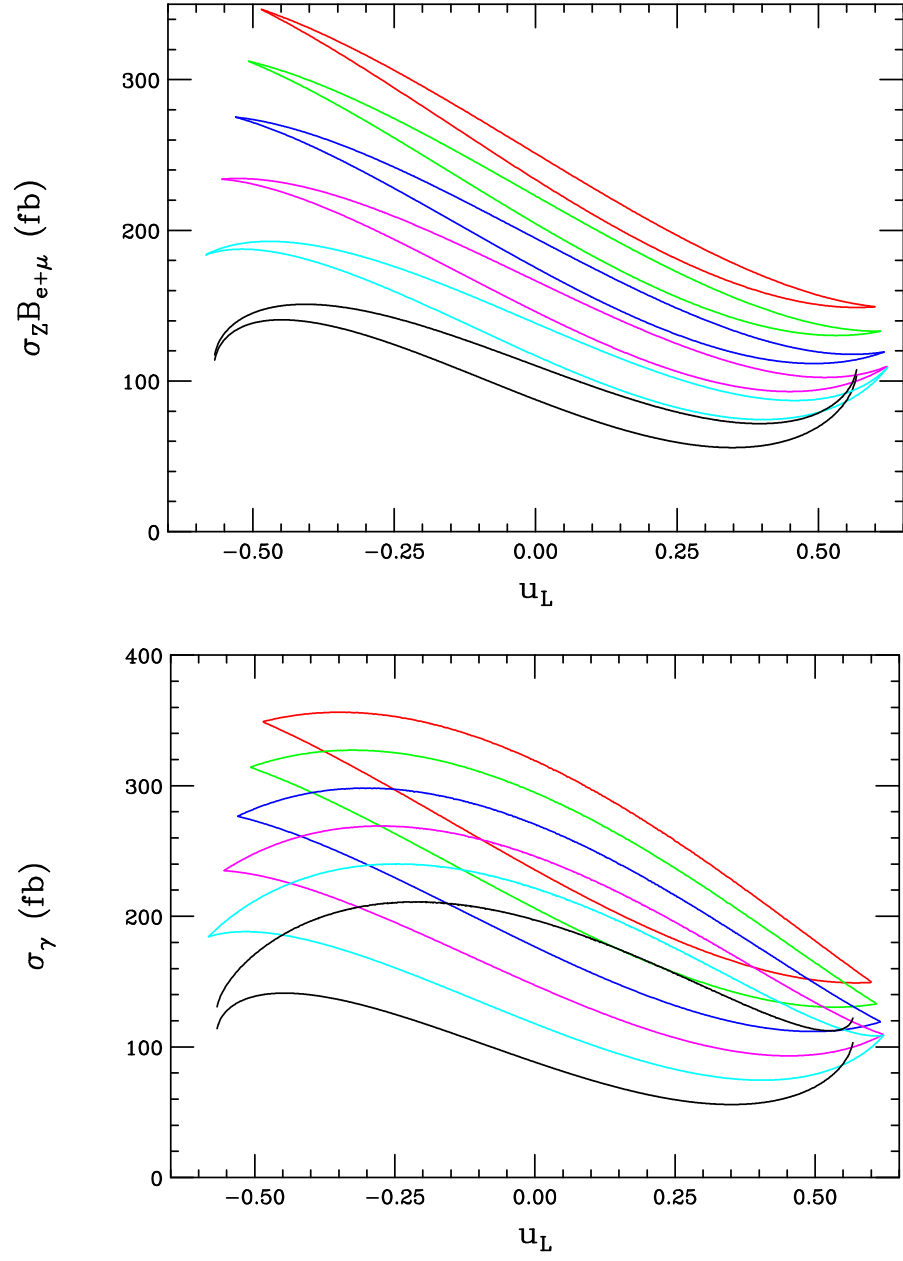


Figure 4: Same as the previous Figure but now for the LHC.

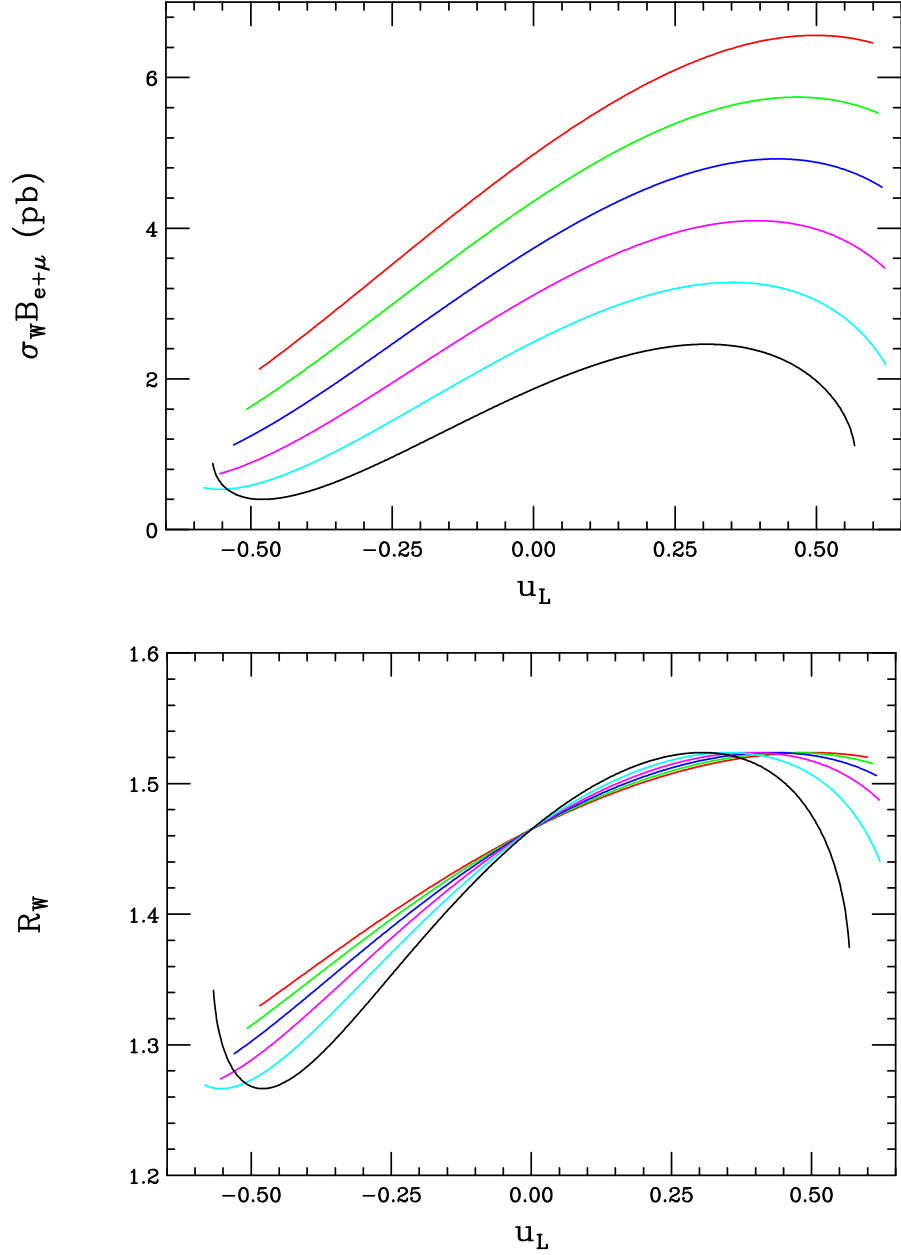


Figure 5: (Top) The predicted values for the sum of the cross section for $W^\pm Z'$ at the LHC based on the corresponding cross section observed by CDF at the Tevatron along the parameter space arcs described above. The W leptonic branching fraction is included. Again, note that another set of solutions exist with $u_L \rightarrow -u_L$. (Bottom) The ratio of the $W^+ Z'$ to the $W^- Z'$ cross sections at the LHC, with the same color coding.

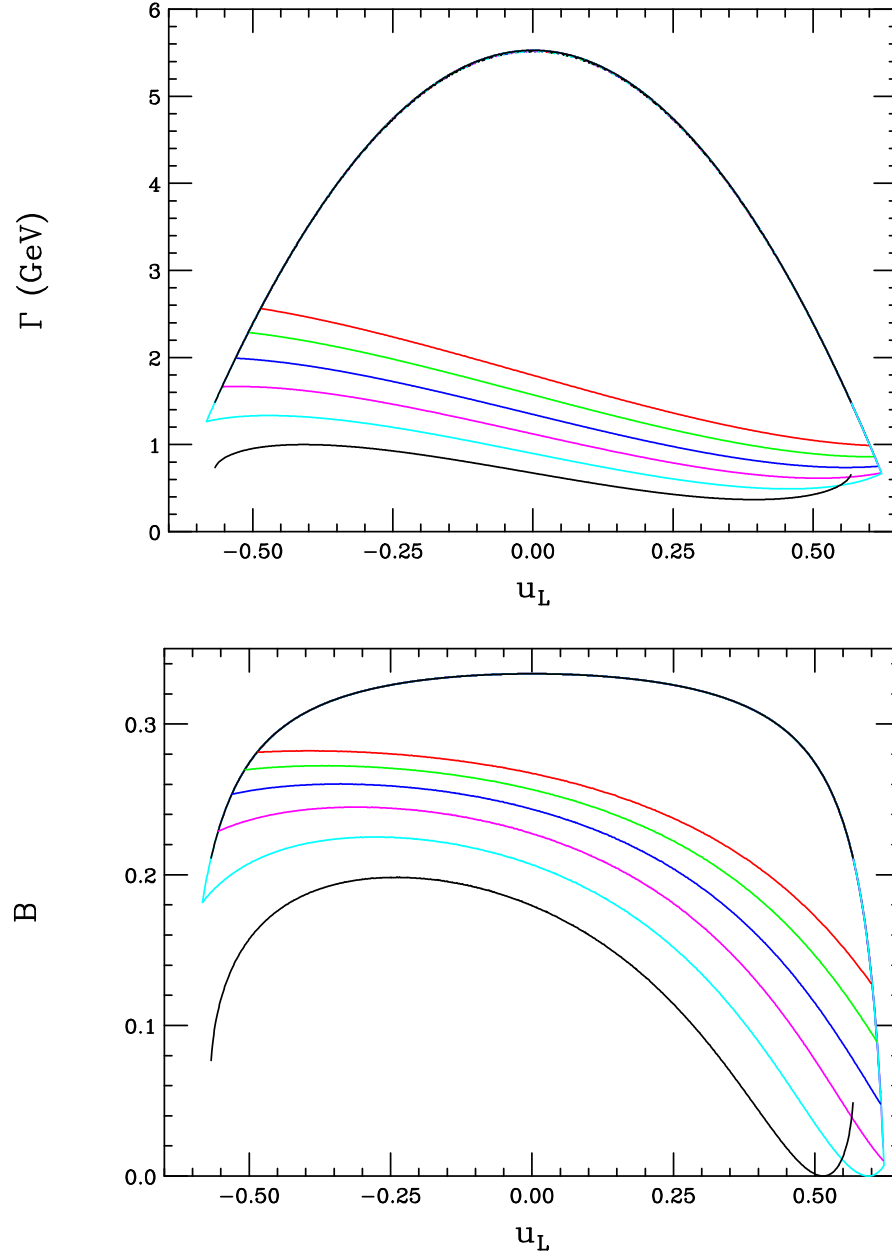


Figure 6: (Top) Predicted ranges for the value of the Z' width, Γ , arising from the parameter space along the color-coded arcs described above. (Bottom) The b -quark branching fraction of the Z' for the corresponding range of coupling parameters.

Since the above analysis restricts the allowed values of u_L, d_L for the new Z' boson (while u_R, d_R play a lesser role and may in fact be zero) one would like to attempt to constrain these couplings further. Clearly a better determination of $\sigma_{WZ'}$ at the Tevatron and a measurement of $\sigma_{\gamma, Z+Z'}$ at both the Tevatron and LHC will be useful in this regard. However, it may be possible to obtain additional information from the $W + Z'$ kinematic distributions themselves. To this end, we return to our discussion of the $W + Z'$ differential cross section above. There, we saw that in the case of $u_L \neq d_L$ an additional term contributes to the cross section, *i.e.*, the term denoted by X , which grows with increasing \hat{s} . If this term is absent, the differential distribution for $d\sigma/dM_{WZ'}$ will peak at low values of $M_{WZ'}$, not far above threshold and then fall rapidly. However, the presence of this term will push this peak in this distribution to significantly larger values of $M_{WZ'}$ and the corresponding fall off of this differential cross section will be far slower. Thus, in principle, a measurement of the $M_{WZ'}$ distribution could provide an additional useful handle on the u_L, d_L coupling relationship which is independent of the values for u_R, d_R .

Since the ‘discovery’ channel, $W^\pm Z'$, has the largest cross section, a detailed study of this reaction can provide us a way to pin down the values of the u_L, d_L couplings which will then further restrict u_R, d_R . In Fig. 7 we show the $d\sigma/dM_{WZ'}$ distribution at the Tevatron and the LHC for several different representative values of u_L, d_L lying within the allowed coupling ellipses shown in Fig. 1. In the top panel for $W + Z'$ production at the Tevatron, we see that this distribution is quite sensitive to the choice of these couplings. In particular, we see that when $u_L = d_L$ the peak in the distribution is at very low $M_{WZ'}$ values, not far from threshold, as expected. However, the peak occurs at larger values of $M_{WZ'}$ when u_L, d_L take on significantly different values. We especially note the strong differences between the cases of $u_L, d_L = (-0.5, 0.5)$ and $u_L, d_L = (-0.5, -0.5)$. Fig. 7 also shows the corresponding results for this distribution at the LHC which show similar coupling sensitivity since the shape of the distributions is quite similar to those found at the Tevatron.

Further information can be obtained by examining other kinematic distributions involving the W^\pm or the dijet system. Fig. 8 shows the angular distribution of the W^\pm at both the Tevatron and the LHC. We notice several things: (i) The $d\sigma/dz$ distribution is very sensitive to the values of the u_L, d_L couplings which can be traced back to the various terms in Eq.(2) above. First, we see that when $u_L = d_L$ the distribution is forward and backward peaked (due to the u - and t -channel ‘poles’) and is $z \rightarrow -z$ symmetric. In the other extreme, where the term proportional to X in Eq.(2) dominates, we still have $z \rightarrow -z$ symmetry but the distribution is much flatter being proportional to $\sim \hat{u}\hat{t}$. In the intermediate cases where all terms are comparable, the $z \rightarrow -z$ symmetry is now lost and some forward and backward peaking is possible. However, the distributions are generally fairly flat for central values of z . (ii) The angular distributions are quite different from what one would expect from scalar production. (iii) As in the case of the $d\sigma/dM_{WZ'}$ spectrum, we note that the W^\pm angular distributions look very similar at both colliders. This will remain true for the other distributions we display below and so we will only show the results for the LHC.

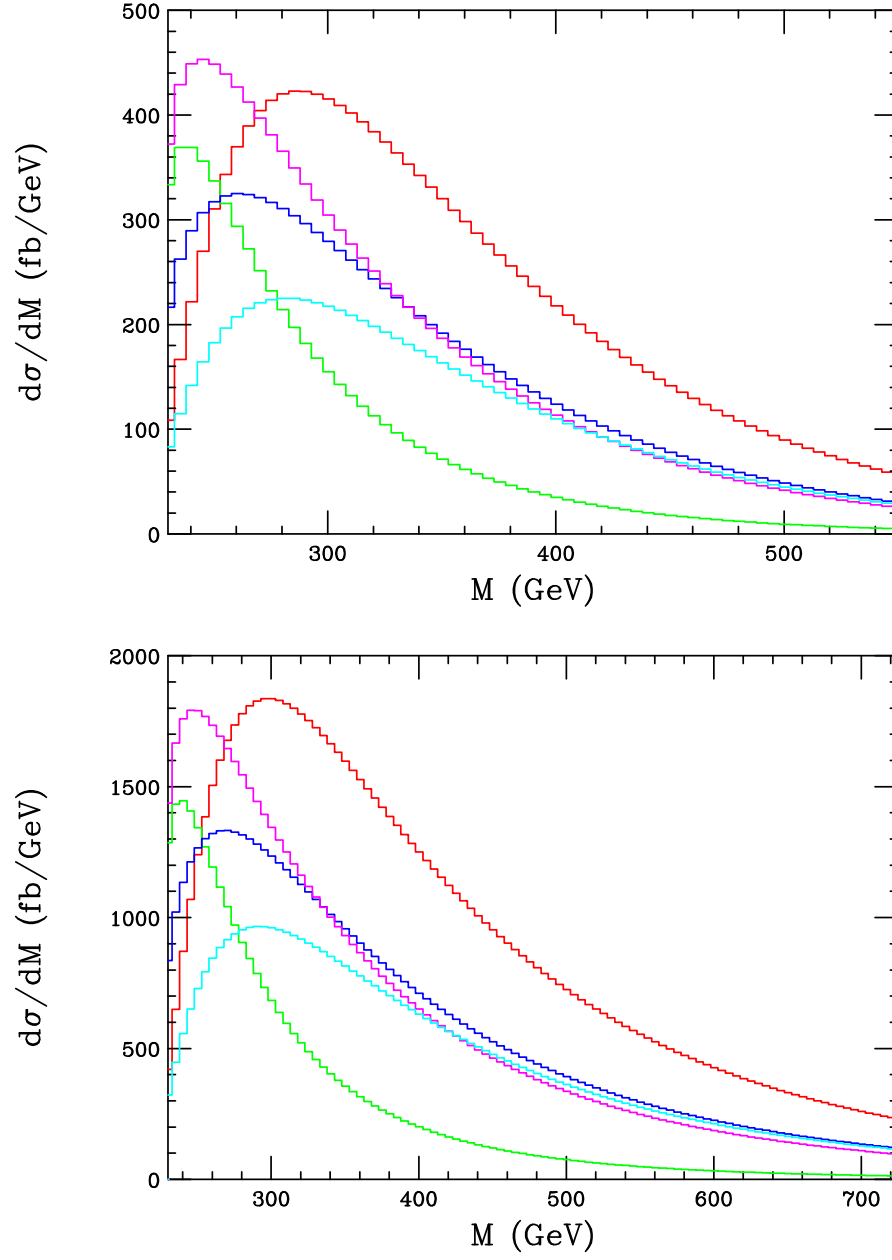


Figure 7: $d\sigma/dM_{WZ'}$ distribution at the Tevatron(top) and LHC(bottom) for several different allowed values of $u_L, d_L = (-0.5, 0.5)$ (red), $(-0.5, -0.5)$ (green), $(0, 0.7)$ (blue), $(-0.2, -0.8)$ (magenta), $(-0.2, 0.5)$ (cyan), respectively.

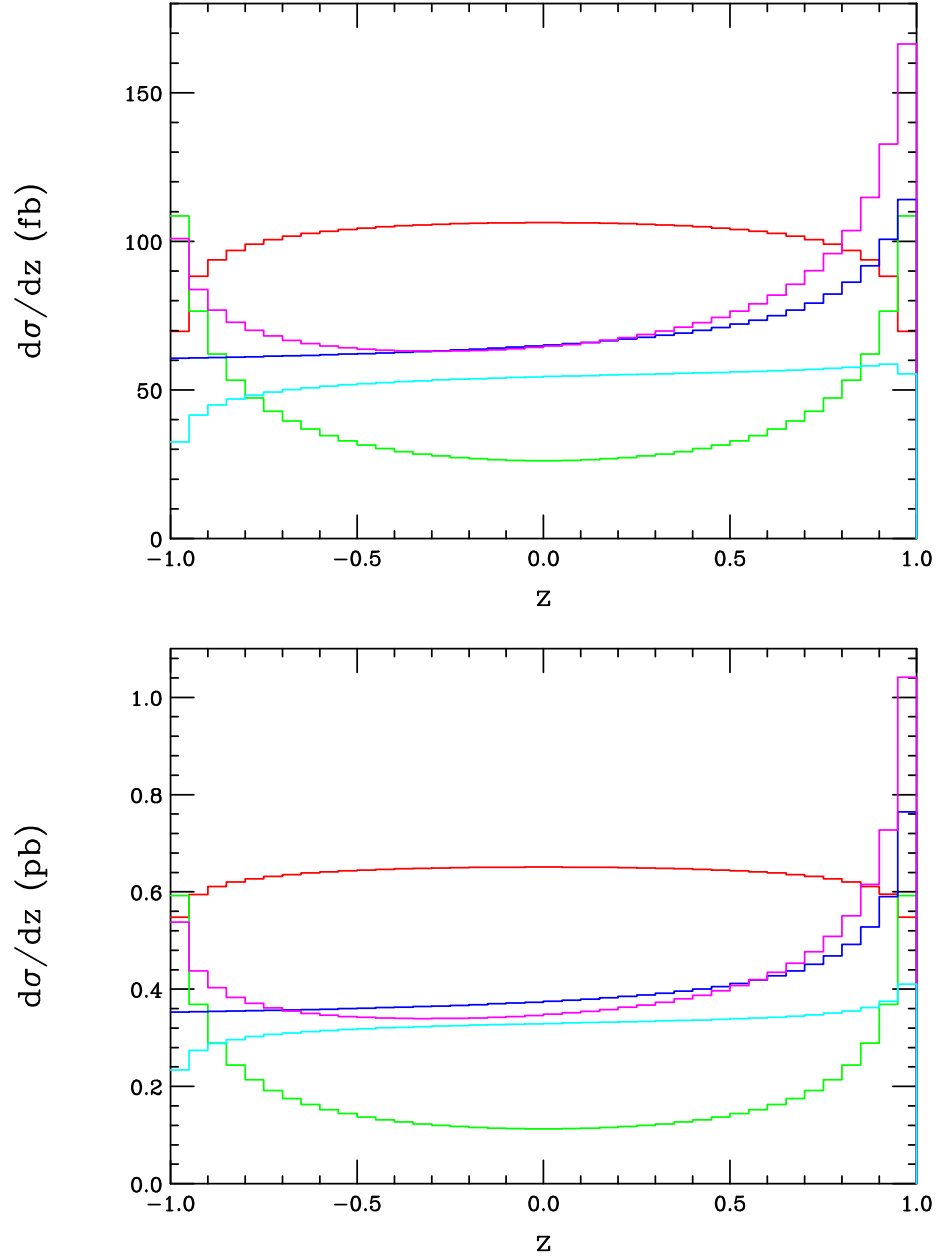


Figure 8: $d\sigma/dz$ ($z = \cos \theta^*$, the CM scattering angle) distributions for the W at the Tevatron(top) and LHC(bottom) for the same set of coupling choices as in the previous figure.

Figure 9 shows both the W^\pm rapidity (y) and p_T distributions at the LHC for the same set of u_L, d_L couplings as examined above. (As noted above, very similar results are obtained at the Tevatron.) The rapidity distribution shows only a relatively weak dependence on the couplings. However, it is easy to see that when $u_L = d_L$ it is quite flat in the central region, whereas, when u_L and d_L are very different it is much more peaked near $y = 0$. On the otherhand, the p_T spectrum of the W^\pm is seen to be highly sensitive to the u_L, d_L couplings as we might have expected based on the shapes of the $d\sigma/dM_{WZ'}$ and the $d\sigma/dz$ distributions discussed above. In particular we see that when $u_L \neq d_L$ the W^\pm p_T spectrum is somewhat harder, growing more so as the difference in couplings gets larger. Clearly information from this distribution will help in the determination of the left-handed quark couplings to the Z' .

Figure. 10 displays the velocity distribution of the Z' in the CM frame; this is of particular importance in the determination of the boost required to go to the dijet CM frame in order to obtain the dijet angular distribution. A measurement of this quantity is necessary if one wants to verify the spin-1 nature of the Z' . Again, we see that this distribution is quite sensitive to the u_L, d_L couplings and peaks at significantly larger values when $u_L \neq d_L$.

Lastly, we have also examined the possibility of observing Z' bremsstrahlung in $q\bar{q}$ production in e^+e^- annihilation, *i.e.*, $e^+e^- \rightarrow q\bar{q}Z'$. We found that the rate for this process is hopelessly small at LEP II energies and thus does not provide a constraint on this scenario.

3 Summary and Conclusions

In summary, we have examined the hypothesis that a leptophobic Z' boson accounts for the excess of events in the Wjj channel as observed by CDF. The quoted range for the production cross section places constraints on the left-handed couplings of the Z' to the up- and down-quarks. Consistency with the lack of observation by D0 forces us to the lower end of this cross section range. Further consistency with the non-observation of dijet resonances at $m_{jj} \sim 150$ GeV at UA2 constrains these couplings, and severely limits the possible values of the Z' right-handed couplings to the light quarks. Assuming that these couplings are generation independent, these results provide a relatively restrictive allowed region for the four hadronic couplings of the Z' .

These allowed coupling regions translate into well-determined rates for the associated production of $Z/\gamma + Z'$ at the Tevatron and LHC, as well as for $W + Z'$ at the LHC, apart from NLO corrections. The Wjj rate at the LHC is large and this channel should be observed soon once the SM backgrounds are under control. The rates for $Z/\gamma + Z'$ associated production are smaller, and these processes should not yet have been observed at the Tevatron given the expected SM backgrounds. Once detected, these processes will provide valuable information on the Z' boson couplings. Further information on the $u_L - d_L$ coupling relationship was shown to also be obtainable from measurements of the $d\sigma/dM_{WZ'}$ as well as other kinematic

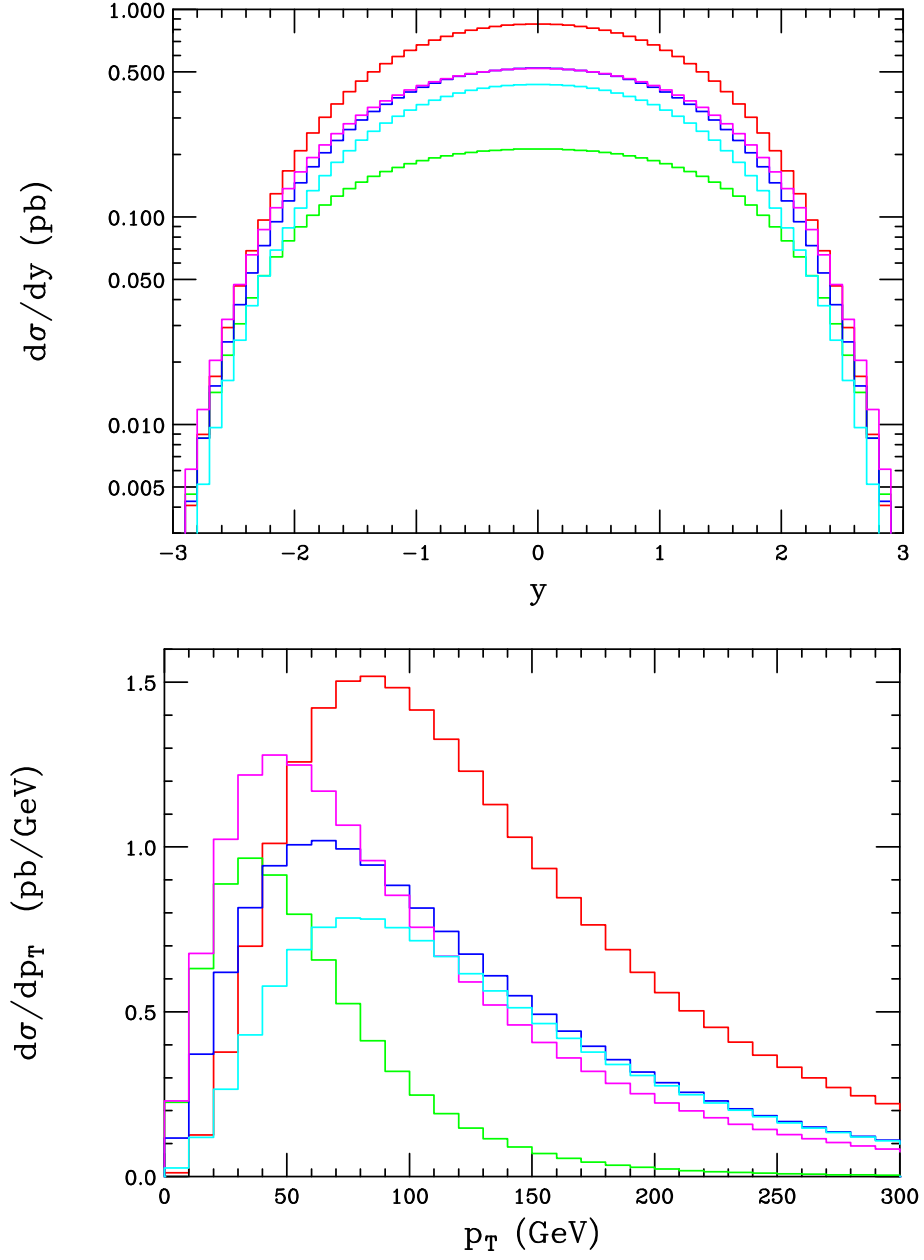


Figure 9: Rapidity (top) and p_T (bottom) distributions for the W^\pm at the LHC for the same set of coupling choices as in the previous figure.

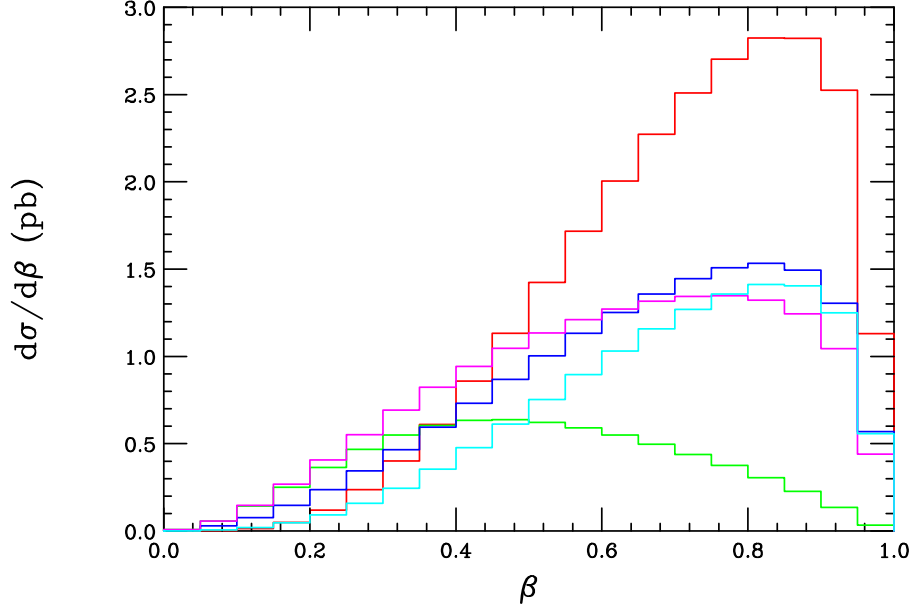


Figure 10: Velocity (β) distribution for the Z' at the LHC in the CM frame for the same set of coupling choices as in the previous figure.

distributions at both the Tevatron and the LHC.

Even with four free coupling parameters, this scenario is predictive, even more so once the $W + Z'$ cross section is better determined at the Tevatron, and can be further tested at both the Tevatron itself as well as at the LHC in the near future. In particular, the LHC should confirm (or not) this scenario soon.

Acknowledgments

The authors would like to thank Viviana Cavaliere for discussions and for answering so many of our questions about the CDF Wjj analysis. The authors would also like to thank Yang Bai for discussions about the Wjj distributions.

References

- [1] T. Aaltonen *et al.* [CDF Collaboration], Phys. Rev. Lett. 106, **171801** (2011). [arXiv:1104.0699 [hep-ex]].
- [2] G. Punzi, talk presented at the *23th Recontres de Blois*, Blois, France, May 2011. See also, http://www-cdf.fnal.gov/physics/ewk/2011/wjj/7_3.html for the latest update of the CDF analysis.
- [3] Z. Sullivan, A. Menon, [arXiv:1104.3790 [hep-ph]]; T. Plehn, M. Takeuchi, [arXiv:1104.4087 [hep-ph]].
- [4] For an updated theoretical analysis using MCFM at NLO, see J. M. Campbell, A. Martin, C. Williams, [arXiv:1105.4594 [hep-ph]].
- [5] M. R. Buckley, D. Hooper, J. Kopp, E. Neil, [arXiv:1103.6035 [hep-ph]]; F. Yu, [arXiv:1104.0243 [hep-ph]]; P. Ko, Y. Omura, C. Yu, [arXiv:1104.4066 [hep-ph]]; D. -W. Jung, P. Ko, J. S. Lee, [arXiv:1104.4443 [hep-ph]]; Z. Liu, P. Nath, G. Peim, [arXiv:1105.4371 [hep-ph]]; M. R. Buckley, D. Hooper, J. Kopp, A. Martin and E. T. Neil, arXiv:1107.5799 [hep-ph].
- [6] X. -P. Wang, Y. -K. Wang, B. Xiao, J. Xu, S. -h. Zhu, [arXiv:1104.1161 [hep-ph]]; K. Cheung, J. Song, [arXiv:1104.1375 [hep-ph]]; L. A. Anchordoqui, H. Goldberg, X. Huang, D. Lust, T. R. Taylor, [arXiv:1104.2302 [hep-ph]]; M. Buckley, P. Fileviez Perez, D. Hooper, E. Neil, [arXiv:1104.3145 [hep-ph]].
- [7] E. J. Eichten, K. Lane, A. Martin, [arXiv:1104.0976 [hep-ph]].
- [8] C. Kilic, S. Thomas, [arXiv:1104.1002 [hep-ph]]; R. Sato, S. Shirai, K. Yonekura, Phys. Lett. **B700**, 122-125 (2011). [arXiv:1104.2014 [hep-ph]].
- [9] X. -P. Wang, Y. -K. Wang, B. Xiao, J. Xu, S. -h. Zhu, [arXiv:1104.1917 [hep-ph]]; B. A. Dobrescu, G. Z. Krnjaic, [arXiv:1104.2893 [hep-ph]]; L. M. Carpenter, S. Mantry, [arXiv:1104.5528 [hep-ph]]; T. Enkhbat, X. -G. He, Y. Mimura, H. Yokoya, [arXiv:1105.2699 [hep-ph]].

- [10] J. A. Aguilar-Saavedra, M. Perez-Victoria, [arXiv:1104.1385 [hep-ph]]; X. -G. He, B. -Q. Ma, [arXiv:1104.1894 [hep-ph]]; A. E. Nelson, T. Okui, T. S. Roy, [arXiv:1104.2030 [hep-ph]]; S. Jung, A. Pierce, J. D. Wells, [arXiv:1104.3139 [hep-ph]]; G. Zhu, [arXiv:1104.3227 [hep-ph]]; P. J. Fox, J. Liu, D. Tucker-Smith, N. Weiner, [arXiv:1104.4127 [hep-ph]]; S. Chang, K. Y. Lee, J. Song, [arXiv:1104.4560 [hep-ph]]; H. B. Nielsen, [arXiv:1104.4642 [hep-ph]]; B. Bhattacharjee, S. Raychaudhuri, [arXiv:1104.4749 [hep-ph]]; Q. -H. Cao, M. Carena, S. Gori, A. Menon, P. Schwaller, C. E. M. Wagner, L. -T. Wang, [arXiv:1104.4776 [hep-ph]]; K. S. Babu, M. Frank, S. K. Rai, [arXiv:1104.4782 [hep-ph]]; B. Dutta, S. Khalil, Y. Mimura, Q. Shafi, [arXiv:1104.5209 [hep-ph]]; J. E. Kim, S. Shin, [arXiv:1104.5500 [hep-ph]]; Z. Usbov, [arXiv:1105.0969 [hep-ph]]; C. -H. Chen, C. -W. Chiang, T. Nomura, Y. Fusheng, [arXiv:1105.2870 [hep-ph]].
- [11] V. M. Abazov *et al.* [D0 Collaboration], [arXiv:1106.1921 [hep-ex]].
- [12] T. G. Rizzo, [hep-ph/0610104]; J. L. Hewett, T. G. Rizzo, Phys. Rept. **183**, 193 (1989).
- [13] V. Cavaliere, CDF Collaboration, private communication.
- [14] T. G. Rizzo, Phys. Rev. **D47**, 956-960 (1993). [hep-ph/9209207]; M. Cvetič, P. Langacker, Phys. Rev. **D46**, 4943 (1992). [hep-ph/9207216].
- [15] R. W. Brown, K. O. Mikaelian, Phys. Rev. **D19**, 922 (1979).
- [16] R. W. Brown, D. Sahdev, K. O. Mikaelian, Phys. Rev. **D20**, 1164 (1979).
- [17] J. L. Hewett, T. G. Rizzo, Phys. Rev. **D47**, 4981-4990 (1993). [hep-ph/9206221].
- [18] P. M. Nadolsky, H. -L. Lai, Q. -H. Cao, J. Huston, J. Pumplin, D. Stump, W. -K. Tung, C. -P. Yuan, Phys. Rev. **D78** (2008) 013004. [arXiv:0802.0007 [hep-ph]].
- [19] J. Alitti *et al.* [UA2 Collaboration], Z. Phys. **C49** (1991) 17-28 and Nucl. Phys. **B400** (1993) 3-24.